REPORT DOCUMENTATION PAGE

Form Approved
OMB No. 0704-0188

1. REPORT DATE *(DD-MM-YYYY)*	**2. REPORT TYPE**	**3. DATES COVERED** *(From - To)*
2006	Journal Article PREPRINT	2005

4. TITLE AND SUBTITLE
Effect of electron-electron scattering on the conductance of a quantum wire (PREPRINT)

5a. CONTRACT NUMBER

5b. GRANT NUMBER

5c. PROGRAM ELEMENT NUMBER

6. AUTHOR(S)
S.K. Lyo and *Danhong Huang

5d. PROJECT NUMBER

5e. TASK NUMBER

5f. WORK UNIT NUMBER

7. PERFORMING ORGANIZATION NAME(S) AND ADDRESS(ES) AND ADDRESS(ES)
Sandia National Laboratories
1515 Eubank Blvd SE
Albuquerque, NM 87185-5800

8. PERFORMING ORGANIZATION REPORT NUMBER

9. SPONSORING / MONITORING AGENCY NAME(S) AND ADDRESS(ES)
*Air Force Research Laboratory
Space Vehicles
3550 Aberdeen Ave SE
Kirtland AFB, NM 87117-5776

10. SPONSOR/MONITOR'S ACRONYM(S)

11. SPONSOR/MONITOR'S REPORT NUMBER(S)
AFRL-VS-PS-JA-2006-1002

12. DISTRIBUTION / AVAILABILITY STATEMENT
Approved for public release; distribution is unlimited. (VS06-0029)

13. SUPPLEMENTARY NOTES
Submitted for publication in Physical Review B
Government Purpose Rights

14. ABSTRACT
Electron-electron scattering conserves total momentum and does not dissipate momentum directly in a low-density system where the Umklapp process is forbidden. However, it can still affect the conductance through the energy relaxation of the electrons. We show here that this effect can be studied with arbitrary accuracy in a multi-sublevel one-dimensional single quantum wire system in the presence of roughness and phonon scattering using a formally exact solution of the Boltzmann transport equation. The intrasubband electron-electron scattering is found to yield no net effect on the transport of electrons in 1D with only one sublevel occupied. For a system with a multi-level occupation, however, we find a significant effect of inter-sublevel electron-electron scattering on the temperature and density dependence of the resistance at low temperatures.

15. SUBJECT TERMS
Space Vehicles, Electron-Electron Scattering, Conductance, Quantum Wire, Boltzmann Transport Equation

16. SECURITY CLASSIFICATION OF:			**17. LIMITATION OF ABSTRACT**	**18. NUMBER OF PAGES**	**19a. NAME OF RESPONSIBLE PERSON**
a. REPORT	**b. ABSTRACT**	**c. THIS PAGE**			Dave A. Cardimona
Unclassified	Unclassified	Unclassified	Unlimited	27	**19b. TELEPHONE NUMBER** *(include area code)* 505-846-5807

Effect of electron-electron scattering on the conductance of a quantum wire

S. K. Lyo

Sandia National Laboratories, Albuquerque, New Mexico 87185

Danhong Huang

Air Force Research Laboratory (AFRO/VSSS), Kirtland Air Force Base, New Mexico 87117

(March 20, 2006)

Abstract

Electron-electron scattering conserves total momentum and does not dissipate momentum directly in a low-density system where the Umklapp process is forbidden. However, it can still affect the conductance through the energy relaxation of the electrons. We show here that this effect can be studied with arbitrary accuracy in a multi-sublevel one-dimensional single quantum wire system in the presence of roughness and phonon scattering using a formally exact solution of the Boltzmann transport equation. The intrasubband electron-electron scattering is found to yield no net effect on the transport of electrons in 1D with only one sublevel occupied. For a system with a multi-level occupation, however, we find a significant effect of inter-sublevel electron-electron scattering on the temperature and density dependence of the resistance at low temperatures.

PACS: 72.20.My, 73.40.Gk, 72.20.Fr, 73.40.Kp

I. INTRODUCTION

Carrier transport in low-dimensional semiconductor structures (quantum wells and wires) is of interest for fast (high mobility) electronic devices. Many previous studies have focused on the low-temperature conduction in semiconductor quantum wires.[1–12] The scope of these past investigations covers fields of low-temperature elastic scattering,[1–8] inelastic scattering,[10,11] and magnetic-field effects[5,6,8–10,12] in quantum wires. In these quantum-wire systems, scattering by impurities, interface roughness at low temperatures and by phonons at high temperatures plays a dominant role for the momentum relaxation of drifting electrons. Although electron-electron scattering has been known to affect the carrier transport in semiconductors for a long time,[13–15] it has not received sufficient attention in the past, especially in the recent calculations of mobilities in semiconductor quantum-wire systems, due to the complexity of calculations involved. In this paper, we examine the effect of electron-electron scattering on the resistivity using the Fermi liquid model. As is well known, electron-electron interaction yields the Lüttinger liquid effect in clean systems. This effect will not be considered here.

In modulation n-doped quantum-wire structures, there are usually many more conduction electrons than ionized impurities inside the channel. As a result, an electron can be scattered much more frequently by other electrons than by ionized impurities, leading to an enhanced effect of electron-electron scattering. In addition, acoustic phonon scattering is suppressed at low temperatures.[10,11] Therefore, electron-electron scattering cannot be ignored in the calculation of the conductance in modulation-doped quantum wires. However, electron-electron scattering alone does not produce momentum dissipation directly because of two-particle momentum conservation.[16] The major role of electron-electron scattering is the energy relaxation where carriers undergo rapid inelastic transitions among all the states accessible by electron-electron scattering. As a result, the momentum relaxation rate becomes averaged over many states, becoming less dependent on the energy, and is driven from the original exact relaxation rate for the rest of the elastic and inelastic scattering

mechanisms without electron-electron scattering. This effect increases the resistivity. A quantitative argument based on the variational principle was given earlier for this effect.[15] In this paper, we quantitatively study the effect of the competition of elastic, inelastic and electron-electron scattering as functions of the temperature T and the electron density n_{1D}.

The intrasubband electron-electron scattering is found to yield no net effect on the transport of electrons in the 1D limit where only one sublevel is occupied. This is in sharp contrast to a finite intrasubband electron-electron scattering in the 2D limit.[15] In multi-sublevel quantum wires, intersubband electron-electron scattering is found to be significant at low temperatures in momentum-relaxation processes as will be demonstrated later in our numerical calculations. It is prohibitively difficult to study the effect of electron-electron scattering in two and three dimensions accurately. In a one dimensional system, however, we can develop an accurate solution to the Boltzmann transport equation utilizing the fact that there are only a discrete number of points in k space for a given energy unlike in higher dimensions.

We establish a matrix-equation approach for numerical calculation. This approach has the advantage of performing numerical calculation with any desired accuracy. As a result, the Boltzmann transport equation (described in the next section) can be solved exactly formally for quantum wires yielding accurate numerical results. We apply this approach to study the temperature- and density-dependent resistance of a single quantum wire. For elastic scattering, we consider only surface-roughness scattering and neglect scattering from ionized impurities by assuming that dopants sit far away from the quantum wire in the growth (z) direction in modulation-doped systems. We study only high-quality quantum wires where the localization length is expected to be longer than the sample length.

The outline of this paper is as follows. In Sec. II we derive an expression for the conductance in the presence of interface-roughness, phonon and electron-electron scattering in a multi-sublevel single quantum wire. In Sec. III we construct a matrix-equation approach

for solving the Boltzmann transport equation numerically with any desired accuracy. In Sec. IV effects of intersubband electron-electron scattering on the temperature and density dependence of the resistance are computed numerically, along with detailed discussions and explanations of the numerical results. A brief conclusion is given in Sec. V.

II. SCATTERING EFFECTS ON MULTI-SUBLEVEL TRANSPORT

In this section, we briefly review the key results in our previous studies [8,10] and repeat some of the equations for completeness of the theory presented in this paper. By using notation nearly identical to that already in the literatures, [8,10] the Boltzmann transport equation for electrons along the wire (y) direction is given by

$$v_j + \frac{2\pi}{\hbar} \sum_{j'} |I_{j',j}|^2 (g_{j'} - g_j)\, \delta(\varepsilon_j - \varepsilon_{j'}) + P_j + Q_j = 0 \ , \tag{1}$$

where P_j stands for the electron-phonon scattering and Q_j represents electron-electron scattering. These quantities will be given below. In Eq. (1), ε_j and $v_j = \hbar^{-1} d\varepsilon_j/dk$ are the kinetic energy and the group velocity of the electrons in the electronic state $j = \{n,\ k\}$. Here, $n = 0,\ 1,\ \cdots$ represents the sublevel index due to the size quantization of the wire in the x direction and k is the wave number of free electrons along the y direction. Moreover, $I_{j',j}$ is the elastic scattering matrix [8] due to interface roughness. The quantity g_j is proportional to the nonequilibrium deviation from the equilibrium Fermi distribution function $f_j^{(-)} \equiv f_0(\varepsilon_j)$ after a linear expansion of the distribution function to the leading order in the external electric field E: $f_j = f_j^{(-)} + g_j[-\partial f_0(\varepsilon_j)\partial\varepsilon_j]eE$.

The quantity P_j in Eq. (1), representing the contribution from the inelastic electron-phonon interaction, is given by [10,17]

$$P_j = \frac{2\pi}{\hbar} \sum_{j',s,\vec{q},\pm} \left|V_{j',j}^{s\vec{q}}\right|^2 \left(f_{j'}^{(\mp)} + n_{s\vec{q}}\right)(g_{j'} - g_j)\ \delta(\varepsilon_j - \varepsilon_{j'} \pm \hbar\omega_{s\vec{q}})\, \delta_{k',\ k\pm q_y} \ , \tag{2}$$

where $V_{j',j}^{s\vec{q}}$ is the screened electron-phonon interaction [11] defined by $< n'k' \left|V_{s,\vec{q}}^{\rm e-ph}\right| nk >= V_{j',j}^{s\vec{q}}\ \delta_{k',\ k+q_y}$ and the sign $-$ (or $+$) corresponds to the one-phonon emission (or absorption)

process. In Eq. (2), $f_{j'}^{(+)} \equiv 1 - f_{j'}^{(-)}$ and $n_{s\vec{q}}$ is the Boson distribution function for phonons of mode s, having wave vector $\vec{q} = (q_x, q_y, q_z)$ and equilibrium phonon energy $\hbar\omega_{s\vec{q}}$.

To consider the effect of electron-electron scattering on transport we assume that only the quantum-well ground state $\phi_0(z)$ with energy level E_{1z} is relevant in the z direction due to an extra-thin thickness of the wire in this direction and low temperatures. The wave function along the wire direction is just a plane wave. The wave function of the nth sublevel in the x direction is denoted by $\psi_n(x)$. We further assume that the confining potential in the x direction is a parabolic confinement. This gives rise to a harmonic wave function $\psi_n(x) = (\alpha/\sqrt{\pi}2^n n!)^{1/2} \exp(-\alpha^2 x^2/2) H_n(\alpha x)$ and a quantized energy level $(n + 1/2)\hbar\Omega_0$, where $H_n(x)$ is the nth-order Hermite polynomial, $\alpha = \sqrt{m^*\Omega_0/\hbar}$, m^* is the effective mass of electrons, and $\hbar\Omega_0$ is the energy-level separation. An electron in an initial state $j = (n,\ k)$ will be scattered into a final state $j' = (n',\ k')$ by simultaneously scattering another electron from an initial state $j_1 = (n_1,\ k_1)$ into a final state $j_1' = (n_1',\ k_1')$ through the Coulomb interaction between two electrons, which is given by

$$K_{j,j_1}^{j',j_1'} = \frac{e^2}{\epsilon_0\epsilon_{\rm r}L^2} \int d^3r\ \phi_0^2(z)\ \psi_{n'}^*(x)\psi_n(x)\ \exp\left[i\left(k - k'\right)y\right]$$

$$\times \int d^3r_1\ \phi_0^2(z_1)\ \psi_{n_1'}^*(x_1)\psi_{n_1}(x_1)\ \frac{\exp\left[i\left(k_1 - k_1'\right)y_1\right]}{|\vec{r} - \vec{r}_1|}\ ,$$

where $\epsilon_{\rm r}$ is the dielectric constant of the host material and L is the wire length. This can be explicitly calculated as

$$K_{j,j_1}^{j',j_1'} = \frac{e^2}{\epsilon_0\epsilon_{\rm r}L}\ \delta_{q_y,\ k_1-k_1'}\delta_{k+k_1,\ k'+k_1'} \int dx \int dz\ \phi_0^2(z)\ \psi_{n'}^*(x)\psi_n(x)$$

$$\times \int dx_1 \int dz_1\ \phi_0^2(z_1)\ \psi_{n_1'}^*(x_1)\psi_{n_1}(x_1) \int dy\ \frac{\exp\left(iq_y y\right)}{\sqrt{\mathcal{R}^2 + y^2}}\ ,$$

and is further simplified to

$$K_{j,j_1}^{j',j_1'} = \delta_{k+k_1,\ k'+k_1'}\ \left(\frac{2e^2}{\epsilon_0\epsilon_{\rm r}L}\right)$$

$$\times \int dx \int dz \int dx_1 \int dz_1 \; K_0\left(|k'-k|\,\mathcal{R}\right) \; \phi_0^2(z)\psi_{n'}^*(x)\psi_n(x) \; \phi_0(z_1)^2\psi_{n_1'}^*(x_1)\psi_{n_1}(x_1) \; , \qquad (3)$$

where $K_0(x)$ is the modified Bessel function of the third kind, and $\mathcal{R} = \sqrt{(z_1-z)^2+(x_1-x)^2}$. By denoting the two-electron wave function as

$$\Psi(j,\; j_1) = \psi_n(x)\frac{\exp\left(iky\right)}{\sqrt{L}} \; \psi_{n_1}(x_1)\frac{\exp\left(ik_1y_1\right)}{\sqrt{L}} \; ,$$

the matrix element of the Coulomb interaction V_c for the normalized spin singlet (upper sign) and the spin triplet (lower sign) states is given by

$$\frac{1}{2} < \Psi(j',j_1') \pm \Psi(j_1',j') \left|V_c\right| \Psi(j,j_1) \pm \Psi(j_1,j) >$$

$$= < \Psi(j',j_1') \left|V_c\right| \Psi(j,j_1) > \pm < \Psi(j_1',j') \left|V_c\right| \Psi(j,j_1) > \; .$$

Here, the first term corresponds to Eq. (3) and the second (*i.e.,* the exchange) term is found by interchanging $j' \leftrightarrow j_1'$. The interaction averaged over the spin configuration leads to

$$\bar{K}_{j,j_1}^{j',j_1'} = K_{j,j_1}^{j',j_1'} - \frac{1}{2} \; K_{j,j_1}^{j_1',j'} \; . \qquad (4)$$

The electron-electron scattering adds a term Q_j on the left hand side of Eq. (1),[18,19] which is given by

$$Q_j = \frac{4\pi}{\hbar k_{\rm B} T} \; \left[-\frac{\partial f_j^{(-)}}{\partial \varepsilon_j}\right]^{-1} \sum_{j',j_1,j_1'} \left|\bar{K}_{j,j_1}^{j',j_1'}\right|^2 \; f_j^{(-)} f_{j_1}^{(-)} f_{j'}^{(+)} f_{j_1'}^{(+)}$$

$$\times \left(g_{j'} + g_{j_1'} - g_j - g_{j_1}\right) \; \delta\left(\varepsilon_j + \varepsilon_{j_1} - \varepsilon_{j'} - \varepsilon_{j_1'}\right) \; . \qquad (5)$$

Here, T is the temperature of the thermal-equilibrium system, and the spin degeneracy has been taken into account. The dynamical screening to the electron-electron scattering in Eq. (5) can be included through the following substitutions

$$\left\{K_{j,j_1}^{j',j_1'},\; K_{j,j_1}^{j_1',j'}\right\} \rightarrow \left\{\frac{K_{j,j_1}^{j',j_1'}}{\epsilon_{j'j}^{\rm RPA}[|k'-k|,\; (\varepsilon_{j'}-\varepsilon_j)/\hbar]},\; \frac{K_{j,j_1}^{j_1',j'}}{\epsilon_{j_1'j}^{\rm RPA}[|k_1'-k|,\; (\varepsilon_{j_1'}-\varepsilon_j)/\hbar]}\right\} \; ,$$

where $\epsilon_{ij}^{\rm RPA}(|q_y|,\; \omega)$ can be found from diagonal elements of a dielectric-function matrix under a random-phase approximation (RPA).[20] After the Fourier transform of $K_0(x)$ with respect to η, the expression for q_y-dependent $K_{j,j_1}^{j',j_1'}$ in Eq. (3) is found to be

$$K^{j',j'_1}_{j,j_1}(q_y) = \delta_{k+k_1,\ k'+k'_1}\ \left(\frac{2e^2}{\epsilon_0\epsilon_{\rm r}L}\right)\ \sqrt{\frac{n^<!n_1^<!}{n^>!n_1^>!}}\ \int_0^{+\infty} d\eta\ \frac{F(\eta,\ q_y)}{\sqrt{\eta^2+q_y^2}}$$

$$\times(-P)^{(n^>-n^<+n_1^>-n_1^<)/2}\exp(-P)L_{n^<}^{(n^>-n^<)}(P)L_{n_1^<}^{(n_1^>-n_1^<)}(P)$$

$$\times\left(\delta_{n^>-n^<,\,\rm even}\ \delta_{n_1^>-n_1^<,\,\rm even}-2\delta_{n^>-n^<,\,\rm odd}\ \delta_{n_1^>-n_1^<,\,\rm odd}\right)\ ,$$

where $q_y = k'-k$, $L_n^{(s)}(x)$ is the nth-order associated Laguerre polynomial, $n^< = \min(n,\ n')$, $n^> = \max(n,\ n')$, $n_1^< = \min(n_1,\ n'_1)$, $n_1^> = \max(n_1,\ n'_1)$, $P = \eta^2/2\alpha^2$, and the form factor is

$$F(\eta,\ q_y) = \int dz \int dz_1\ \phi_0^2(z)\ \exp(-\sqrt{\eta^2+q_y^2}|z-z_1|)\ \phi_0(z_1)^2\ .$$

The conductance is found to be [8]

$$G = \frac{2e^2}{L^2}\ \sum_j\ v_j g_j\ \int_0^{+\infty}\ d\varepsilon\ \delta\left(\varepsilon_j-\varepsilon\right)\ \left[-\frac{\partial}{\partial\varepsilon}f^{(-)}(\varepsilon)\right]$$

$$= \frac{2e^2}{hL}\ \int_0^{+\infty}\ d\varepsilon\ \left[-\frac{\partial}{\partial\varepsilon}f^{(-)}(\varepsilon)\right]\ S^\dagger\otimes\tilde{g}\ , \tag{6}$$

where the symbol $\otimes$ represents the matrix inner product, the k-summation for the running variable j is converted into the ε_j-integration in the second equality, and S, $\tilde{g}$ are column vectors with elements s_ν and $\tilde{g}_\nu$ defined below. The index ν describes a group of discrete equi-energy points given by the intersection of the horizontal line at an energy ε with a series of energy-dispersion curves, namely the solution of $\varepsilon = \varepsilon_j$ for each j. The element $s_\nu = v_\nu/\left|v_\nu\right|$ of the column vector S in Eq. (6) is the sign of the slope of the tangent to the dispersion curves at these points. The quantity $\tilde{g}_\nu$ is related to g_ν at the equi-energy point ν. Enumerating the indices of these points by

$$\nu = -N,\ -N+1,\ \cdots,\ -1,\ 1,\ \cdots,\ N-1,\ N \tag{7}$$

for symmetric dispersion curves, introducing $g_\nu = \tilde{g}_\nu + g_N$, and using the fact that $g_{-\nu} = -g_\nu$, we find [8]

$$g_\nu = \tilde{g}_\nu - \frac{1}{2}\,\tilde{g}_{-N}, \quad \tilde{g}_N \equiv 0. \tag{8}$$

The branch index n and the wave number k of the equi-energy point ν depends on the energy ε. Hereafter, we put this ε-dependence specifically on all quantities, *e.g.*, $g_\nu(\varepsilon)$. Following the previous treatment, [8] we find

$$U(\varepsilon) \otimes \tilde{g}(\varepsilon) + \mathcal{V}^{-1}(\varepsilon) \otimes P(\varepsilon) + \mathcal{V}^{-1}(\varepsilon) \otimes Q(\varepsilon) = -S(\varepsilon)\ . \tag{9}$$

Here $\tilde{g},\ S,\ P$ and Q are column vectors with the index ν excluding the end point $\nu = N$ for each energy ε in Eq. (7), $\mathcal{V}(\varepsilon)$ is a diagonal matrix with absolute velocity $|v|$ being its element in ν, and U is the $2N-1$ by $2N-1$ square matrix (taking away the last row and column) [8] with its off-diagonal elements $(j' \neq j)$ by

$$u_{j',j} = \frac{\alpha \Lambda^2 V_0^2 \delta b^2}{\hbar^2 |v_{j'} v_j|}\ \exp\left[-\frac{1}{4}(k-k')^2\Lambda^2\right] |\phi_0(z_1)|^4$$

$$\times \int_0^{+\infty} d\eta\ \exp(-\eta^2/2) L_n(\eta^2/2) L_{n'}(\eta^2/2)$$

and its diagonal elements by

$$u_{j,j} = -\sum_{j' \neq j}\ u_{j,j'}\ .$$

Here, $L_n(x) \equiv L_n^{(0)}(x)$, z_1 is the position of the $Al_xGa_{1-x}As$/GaAs-interface of a symmetric quantum well in the growth direction, V_0 is the conduction band offset at the interface, δb is the average layer fluctuation, and Λ is the correlation length of roughness in the x, y directions. The elimination of the Nth-point in the process of reducing Eq. (1) into Eq. (9) is necessary due to the fact that the matrix U is singular in general and has no inverse if this point is included. [8]

In order to carry out the $\vec{q}$-summation in Eq. (2) for phonon scattering, we introduce a cylindrical coordinate $q_x = q_\perp \cos\phi$, $q_z = q_\perp \sin\phi$, $q = \sqrt{q_\perp^2 + q_y^2}$ and transform

$$\sum_{\vec{q}} \delta_{q_y,\, k'-k} = \frac{\mathcal{A}}{(2\pi)^2} \int q_\perp dq_\perp \int d\phi \; \delta_{q_y,\, k'-k} = \frac{\mathcal{A}}{(2\pi)^2} \int q dq \int d\phi \; \delta_{q_y,\, k'-k} \; ,$$

where $\mathcal{A}$ is the cross-sectional area of the wire. We now employ the Debye approximation at low temperatures for acoustic phonons and use $\hbar\omega_{s\vec{q}} = \hbar c_s q$, where c_s is the sound velocity. Carrying out the q-integration through the energy delta function and converting the k'-summation into the energy-integration, we find

$$\frac{P_\nu(\varepsilon)}{|v_\nu(\varepsilon)|} = \frac{\Omega}{(2\pi)^2\hbar^2} \sum_{n',s,\pm} \int d\varepsilon' \; \frac{q\Theta\left(\pm\varepsilon' \mp \varepsilon\right)}{\hbar c_s} \int d\phi \; \frac{\left|V^{s\vec{q}}_{j',\nu}(\varepsilon,\varepsilon')\right|^2}{|v_{j'}(\varepsilon')v_\nu(\varepsilon)|}$$

$$\times \left(f^{(\mp)}_{j'} + n_{s\vec{q}}\right) \; \left[g_{j'}(\varepsilon') - g_\nu(\varepsilon)\right] \; , \tag{10}$$

where $\Omega = \mathcal{A}L$ is the sample volume, $\Theta(\varepsilon)$ is the unit step function,

$$\hbar c_s q = \left|\varepsilon_\nu - \varepsilon'_{j'}\right| \; , \quad |q_y| = |k' - k| \; , \quad \text{and} \quad q_\perp = \sqrt{q^2 - q_y^2} \; . \tag{11}$$

In Eq. (10), ε_ν indicates the point ν at the energy ε, and the ε'-integration excludes the region where $q_\perp$ becomes imaginary. The electron-phonon interaction matrix elements in Eq. (10) are calculated as

$$|V^{s\vec{q}}_{n',n}|^2 = \frac{V^2_{s\vec{q}}}{|\epsilon^{\rm RPA}_{n'n}(|q_y|,\omega)|^2} \; \Delta_{n'n}(q_x)\Delta_z(q_z)$$

with $\omega = (\varepsilon_{n',k'} - \varepsilon_{n,k})/\hbar$, where

$$\Delta_{n'n}(q_x) = \frac{n_<!}{n_>!} P_1^m \exp(-P_1)[L^{(m)}_{n_<}(P_1)]^2 \; ,$$

$P_1 = q_x^2/2\alpha^2$, $m = n_> - n_<$, $n_>$ ($n_<$) are the larger (lesser) of n and n', and

$$\Delta_z(q_z) = \left|\int dz \; \exp(iq_z z)\phi_0^2(z)\right|^2 \; .$$

Moreover, for the longitudinal ($s = l$) and transverse ($s = t$) modes of acoustic phonons, we find

$$V_{l\vec{q}}^2 = \frac{\hbar q}{2\Omega\rho_0 c_l}\left[D^2 + (eh_{14})^2\frac{A_l(\vec{q})}{q^2}\right] \ ,$$

$$V_{t\vec{q}}^2 = \frac{\hbar q}{2\Omega\rho_0 c_t}(eh_{14})^2\frac{A_t(\vec{q})}{q^2} \ ,$$

where ρ_0, D, and h_{14} are the ion-mass density, deformation-potential coefficient, and piezoelectric constant [10] and the form factors are

$$A_l(\vec{q}) = \frac{36q_x^2q_y^2q_z^2}{q^6} \ ,$$

$$A_t(\vec{q}) = \frac{2[q^2(q_x^2q_y^2 + q_y^2q_z^2 + q_z^2q_x^2) - 9q_x^2q_y^2q_z^2]}{q^6} \ .$$

By defining

$$\varepsilon_j(k=0) + \varepsilon_{j_1}(k_1=0) - \varepsilon_{j'}(k'=0) - \varepsilon_{j_1'}(k_1'=0) = \frac{\hbar^2\xi}{m^*} \ ,$$

the energy-delta function in Eq. (5) with a parabolic energy dispersion $\varepsilon_j \equiv \varepsilon_{n,k} = E_{1z} + (n+1/2)\hbar\Omega_0 + \hbar^2k^2/2m^*$ can be rewritten as

$$\delta\left(\varepsilon_j + \varepsilon_{j_1} - \varepsilon_{j'} - \varepsilon_{j_1'}\right) = \frac{m^*}{\hbar^2}\,\delta\left[(k'-k)\,(k'-k_1) - \xi\right] \ .$$

Here, ξ is related to the energy-level separation $\hbar\Omega_0$. When both electrons undergo intrasubband scattering, only the exchange scattering with $k' = k_1$ and $k_1' = k$ is possible in view of $\xi = 0$. In this case, however, $Q_j = 0$ because the sum of all g factors in Eq. (5) vanishes. Therefore, the intrasubband electron-electron scattering cancels itself completely and has no net effect on the conductance for a single-sublevel occupation in the 1D limit. In the following, we consider intersubband electron-electron scattering that involves only two occupied sublevels at low densities for simplicity and write $\hbar\Omega_0 \equiv \hbar^2k_\Delta^2/2m^*$. Possible values of ξ are given by $\xi = \delta n k_\Delta^2/2$, where $\delta n = \pm 1, \ \pm 2$, depending on whether only one electron undergoes intersubband scattering or both electrons jump from the same sublevel to the other.

For electron-electron scattering, we now carry out momentum summations in Eq. (5) for the last two terms $\propto g_j + g_{j_1}$ which are denoted by $Q_j^{(-)}$. For this purpose, we write the energy delta function as

$$\delta\left(\varepsilon_j + \varepsilon_{j_1} - \varepsilon_{j'} - \varepsilon_{j_1'}\right) = \frac{m^*}{\hbar^2}\,\delta\left(\left[k' - k_-(k_1,k,\delta n)\right]\left[k' - k_+(k_1,k,\delta n)\right]\right)$$

$$= \frac{m^*\Theta\left[D(k_1-k,\delta n)\right]}{\hbar^2\sqrt{D(k_1-k,\delta n)}}\,\left\{\delta\left[k' - k_-(k_1,k,\delta n)\right] + \delta\left[k' - k_+(k_1,k,\delta n)\right]\right\}\ ,$$

where

$$k_\pm(k_1,k,\delta n) = \frac{1}{2}\left[k_1 + k \pm \sqrt{D(k_1-k,\delta n)}\right],\quad D(k_1-k,\delta n) = (k_1-k)^2 + 2\delta n k_\Delta^2\ , \quad (12)$$

$\delta n = n + n_1 - n' - n_1' \neq 0$. From these, we find

$$Q_j^{(-)} = -\frac{m^*L^2}{\pi\hbar^3 f_j^{(+)}}\sum_{n_1,n',n_1',s=\pm}\int\ dk_1\ \left|\bar{K}_{j,j_1}^{j',j_1'}\right|^2$$

$$\times f_{j_1}^{(-)} f_{j'}^{(+)} f_{j_1'}^{(+)}\ \left(g_j + g_{j_1}\right)\ \frac{\Theta\left[D(k_1-k,\delta n)\right]}{\sqrt{D(k_1-k,\delta n)}}\,\delta_{k_1',\ k_s(k_1,k,\delta n)}\,\delta_{k',\ k_{-s}(k_1,k,\delta n)}\ , \qquad \delta n \neq 0\ . \quad (13)$$

The first two terms $\propto g_{j'} + g_{j_1'}$ in the momentum summations of Eq. (5) are denoted by $Q_j^{(+)}$. Using

$$\delta\left(\varepsilon_j + \varepsilon_{j_1} - \varepsilon_{j'} - \varepsilon_{j_1'}\right) = \frac{m^*}{\hbar^2}\,\delta\left(\left[k_1 - k_-(k',k_1',-\delta n)\right]\left[k_1 - k_+(k',k_1',-\delta n)\right]\right)$$

$$= \frac{m^*\Theta\left[D(k_1'-k',-\delta n)\right]}{\hbar^2\sqrt{D(k_1'-k',-\delta n)}}\,\left\{\delta\left[k_1 - k_-(k',k_1',-\delta n)\right] + \delta\left[k_1 - k_+(k',k_1',-\delta n)\right]\right\}\ ,$$

we find $k_1 = k_\pm(k',k_1',-\delta n)$ and $k = k_\mp(k',k_1',-\delta n)$. The expression for k yields

$$k_1' = k - \frac{\delta n k_\Delta^2}{2(k'-k)} \quad \rightleftharpoons \quad k' = k - \frac{\delta n k_\Delta^2}{2(k_1'-k)}\ . \quad (14)$$

Based on these, we arrive at

$$Q_j^{(+)} = \frac{m^*L^2}{\pi\hbar^3 f_j^{(+)}}\sum_{n_1,n',n_1',s=\pm}\left\{\int\ dk'\ g_{j'}\ \delta_{k_1',\ k-\delta n k_\Delta^2/[2(k'-k)]} + \int\ dk_1'\ g_{j_1'}\ \delta_{k',\ k-\delta n k_\Delta^2/\left[2(k_1'-k)\right]}\right\}$$

$$\times \left|\bar{K}^{j',j'_1}_{j,j_1}\right|^2 \; f^{(-)}_{j_1} f^{(+)}_{j'} f^{(+)}_{j'_1} \; \frac{\Theta\left[D(k'_1-k',-\delta n)\right]}{\sqrt{D(k'_1-k',-\delta n)}} \; \delta_{k_1,\; k_s(k',k'_1,-\delta n)}, \qquad \delta n \neq 0 \; . \tag{15}$$

We now interchange variables $j' \longleftrightarrow j_1$ for the k'-integration and variables $j'_1 \longleftrightarrow j_1$ for the k'_1-integration in Eq. (15), and obtain

$$Q^{(+)}_j = \frac{m^* L^2}{\pi\hbar^3 f^{(+)}_j} \sum_{n_1,n',n'_1,s=\pm} \int \; dk_1 \; g_{j_1}$$

$$\times \Bigg\{ \left|\bar{K}^{j_1,j'_1}_{j,j'}\right|^2 \; f^{(+)}_{j_1} f^{(-)}_{j'} f^{(+)}_{j'_1} \; \frac{\Theta\left[D(k'_1-k_1,-\delta n_1)\right]}{\sqrt{D(k'_1-k_1,-\delta n_1)}} \; \delta_{k',\; k_s(k_1,k'_1,-\delta n_1)} \; \delta_{k'_1,\; k-\delta n_1 k^2_\Delta/[2(k_1-k)]}$$

$$+ \left|\bar{K}^{j',j_1}_{j,j'_1}\right|^2 \; f^{(+)}_{j_1} f^{(+)}_{j'} f^{(-)}_{j'_1} \; \frac{\Theta\left[D(k_1-k',-\delta n_2)\right]}{\sqrt{D(k_1-k',-\delta n_2)}} \; \delta_{k'_1,\; k_s(k',k_1,-\delta n_2)} \; \delta_{k',\; k-\delta n_2 k^2_\Delta/[2(k_1-k)]} \Bigg\} \; , \tag{16}$$

where $\delta n_1 = n - n_1 + n' - n'_1 \neq 0$ and $\delta n_2 = n - n_1 - n' + n'_1 \neq 0$.

III. MATRIX FORMALISM FOR THE CONDUCTANCE

In this section, we present details of the matrix formalism for solving the Boltzmann transport equation numerically with any desired accuracy. For the phonon scattering P term, let us first define the scattering-out (second) term on the right-hand side of Eq. (10)

$$W^{(o)}_\nu(\varepsilon) = \frac{\Omega}{(2\pi)^2\hbar^2} \sum_{n',s,\pm} \int \; d\varepsilon' \; \frac{q\Theta\left(\pm\varepsilon' \mp \varepsilon\right)}{\hbar c_s} \int \; d\phi \; \frac{\left|V^{s\vec{q}}_{j',\nu}(\varepsilon,\varepsilon')\right|^2}{|v_\nu(\varepsilon) v_{j'}(\varepsilon')|} \; \left(f^{(\mp)}_{j'} + n_{s\vec{q}}\right) \tag{17}$$

along with conditions given in Eq. (11). We now replace the ε'-integration in the scattering-in (first) term in Eq. (10) by a summation over energy points uniformly spaced with a sufficiently small energy interval $\delta\varepsilon$. We further introduce a new index $t = \{\ell,\; m\}$, where ℓ counts points from the left to the right for a given energy and m indicates energy branches in the above subdivision. Defining

$$W_{t,t'} = \frac{\Omega\delta\varepsilon}{(2\pi)^2\hbar^2} \sum_{s,\pm} \frac{q\Theta\left(\pm\varepsilon' \mp \varepsilon\right)}{\hbar c_s} \int \; d\phi \; \frac{\left|V^{s\vec{q}}_{t',t}\right|^2}{|v_t v_{t'}|} \; \left(f^{(\mp)}_{t'} + n_{s\vec{q}}\right) \; , \tag{18}$$

we can recast Eq. (10) into a matrix form

$$\frac{P_t}{|v_t|} + W_t^{(o)}\ g_t = \sum_{t'}\ W_{t,t'}\ g_{t'} \tag{19}$$

with $W_t^{(o)} = \sum_{t'} W_{t,t'}$. This equation can be rewritten in view of Eq. (8) as

$$\frac{P_t}{|v_t|} = \sum_{t'}\ \tilde{W}_{t,t'}\ \tilde{g}_{t'}, \tag{20}$$

where for $t = \{\ell,\ m\}$ and $t' = \{\ell', m'\}$ we have

$$\tilde{W}_{t,t'} = \left(W_{t,t'} - \delta_{t,t'}\ W_t^{(o)}\right)\ \left(1 - \frac{1}{2}\ \delta_{\ell',1}\right)\ . \tag{21}$$

It is understood that the index t (t') excludes the right-most point for a given energy index m (m'). Here, $\ell' = 1$ signifies the left-most point for any energy index m'.

For the intersubband electron-electron scattering Q term, we now transform the k_1-integration in Eqs. (13) and (16) into an energy integration using $dk_1 = d\varepsilon_{j_1}/\hbar\,|v_{j_1}|$ and change the ε_{j_1}-integration into a discrete summation by chopping the integration into many sufficiently small uniform intervals of width $\delta\varepsilon$ as before. Equation (13) leads to

$$Q_j^{(-)} = -\,|v_j|\ \left(Z_j^{(0)}\ g_j + \sum_{j_1}\ Z_{j,j_1}^{(1)}\ g_{j_1}\right)\ , \tag{22}$$

where $Z_j^{(0)} = \sum_{j_1} Z_{j,j_1}^{(1)}$ and

$$Z_{j,j_1}^{(1)} = -\frac{m^* L^2 \delta\varepsilon}{\pi\hbar^4 f_j^{(+)}}\ \sum_{n',n_1',s=\pm}\ \frac{f_{j_1}^{(-)}}{|v_j v_{j_1}|}\ \left|\bar{K}_{j,j_1}^{j',j_1'}\right|^2$$

$$\times f_{j'}^{(+)} f_{j_1'}^{(+)}\ \frac{\Theta\left[D(k_1-k,\delta n)\right]}{\sqrt{D(k_1-k,\delta n)}}\ \delta_{k_1',\ k_s(k_1,k,\delta n)}\ \delta_{k',\ k_{-s}(k_1,k,\delta n)}\ , \qquad \delta n \neq 0\ . \tag{23}$$

The quantity $Q_j^{(+)}$ in Eq. (16) can also be written in a matrix form

$$Q_j^{(+)} = |v_j|\ \sum_{j_1}\ Z_{j,j_1}^{(2)}\ g_{j_1}\ , \tag{24}$$

where

$$Z_{j,j_1}^{(2)} = \frac{m^* L^2 \delta\varepsilon}{\pi\hbar^4 f_j^{(+)}}\ \sum_{n',n_1',s=\pm} \frac{f_{j_1}^{(+)}}{|v_j v_{j_1}|}\ \left\{\left|\bar{K}_{j,j'}^{j_1,j_1'}\right|^2\ f_{j'}^{(-)} f_{j_1'}^{(+)}\ \frac{\Theta\left[D(k_1'-k_1,-\delta n_1)\right]}{\sqrt{D(k_1'-k_1,-\delta n_1)}}\right.$$

$$\times\delta_{k',\ k_s(k_1,k_1',-\delta n_1)}\ \delta_{k_1',\ k-\delta n_1 k_\Delta^2/[2(k_1-k)]} + \left|\bar{K}^{j',j_1}_{j,j_1'}\right|^2\ f^{(+)}_{j'} f^{(-)}_{j_1'}\ \frac{\Theta\left[D(k_1-k',-\delta n_2)\right]}{\sqrt{D(k_1-k',-\delta n_2)}}$$

$$\times\delta_{k_1',\ k_s(k',k_1,-\delta n_2)}\ \delta_{k',\ k-\delta n_2 k_\Delta^2/[2(k_1-k)]}\Big\}\ , \qquad \delta n_1 \neq 0,\ \delta n_2 \neq 0\ . \tag{25}$$

Finally, the last term on the left side of Eq. (1) is then given by

$$Q_j = |v_j|\ \left(-Z_j^{(0)} g_j + \sum_{j_1}\ Z_{j,j_1}\ g_{j_1}\right) \tag{26}$$

with $Z_{j,j_1} = Z^{(2)}_{j,j_1} - Z^{(1)}_{j,j_1}$, and the summation on j_1 indicates summing over all points generated by intersections between uniformly spaced horizontal energy lines and energy-dispersion curves. Replacing $g_j = \tilde{g}_j - \frac{1}{2}\ \tilde{g}_{-N}$, we obtain

$$\frac{Q_t}{|v_t|} = \sum_{t'}\ \tilde{Z}_{t,t'}\ \tilde{g}_{t'}\ , \tag{27}$$

where for $t = \{\ell,\ m\}$ and $t' = \{\ell',\ m'\}$

$$\tilde{Z}_{t,t'} = \left(Z_{t,t'} - \delta_{t,t'}\ Z_t^{(o)}\right)\ \left(1 - \frac{1}{2}\ \delta_{\ell',1}\right)\ . \tag{28}$$

Inserting Eqs. (20) and (27) into Eq. (9), we find

$$\left[U + \tilde{W} + \tilde{Z}\right] \otimes \tilde{g} = -S\ , \tag{29}$$

and the solution of Eq. (29) is

$$\tilde{g} = -\left[U + \tilde{W} + \tilde{Z}\right]^{-1} \otimes S\ . \tag{30}$$

Here, indices $t = \{\ell, m\}$ and $t' = \{\ell', m'\}$ exclude the right-most points for any given energy indices $m,\ m'$. The index m is the k value at the intersection point t. Note that U is block-diagonal, namely $U_{t,t'} \propto \delta_{m',m}$, while $|v_{t,t'}| \propto \delta_{t,t'}$ is diagonal. When both the roughness and phonon scattering are absent from Eq. (30), *i.e.* $U = \tilde{W} = 0$, we find that the matrix $\tilde{Z}$ itself is singular. This confirms that the electron-electron scattering alone does not contribute to the resistance in the transport due to the fact that it conserves total momentum and does not dissipate momentum. The conductance is found from the discrete version of Eq. (6):

$$G = \frac{2e^2}{hL}\ \delta\varepsilon\ \sum_t\ \left[-\frac{\partial}{\partial\varepsilon_t} f^{(-)}(\varepsilon_t)\right]\ S_t^\dagger \otimes \tilde{g}_t\ . \tag{31}$$

IV. NUMERICAL RESULTS AND DISCUSSION

In this section, we present the numerical results and discussions. In our numerical calculations, we have chosen the following parameters. For the quantum well in the z direction, we employ $m^* = 0.067\ m_0$ in the well (m_0 being the free electron mass), $m_{\rm B} = 0.073\ m_0$ in the barrier, $V_0 = 280\ meV$ for the barrier height, $L_{\rm W} = 50\ \mathring{A}$ for the well width, and $\epsilon_{\rm r} = 12$ for the average dielectric constant. These parameters yield $E_{1{\rm z}} = 84\ meV$ for the ground-state energy and $E_{2{\rm z}} - E_{1{\rm z}} = 188\ meV$ for the energy separation between the first excited level and the ground state. For the parabolic confinement in the x direction, we use $\hbar\Omega_0 = 2.7\ meV$ for the energy-level separation. For the interface roughness, we assume $\delta b = 5\ \mathring{A}$ for the average layer fluctuation in the z direction and $\Lambda = 10\ \mathring{A}$ for the Gaussian correlation length in the x, y directions. For the acoustic phonons in the bulk, the following parameters are employed: $c_l = 5.14 \times 10^5\ cm/s$ for the longitudinal mode, $c_t = 3.04 \times 10^5\ cm/s$ for the transverse mode, $D = -9.3\ eV$ for the deformation potential, $h_{14} = 1.2 \times 10^7\ V/cm$ for the piezoelectric field, and $\rho_0 = 5.3\ g/cm^3$ for the ion mass density. The wire length in the y direction is assumed to be $L = 1\ \mu m$ except for the cases indicated.

For the 1D density $n_{\rm 1D} = 10^6\ cm^{-1}$ assumed for the numerical study, the relative chemical potential $\bar{\mu} = \mu - E_{1{\rm z}} - \hbar\Omega_0/2$ shows that $\hbar\Omega_0 < \bar{\mu} < 2\hbar\Omega_0$ for the temperature range $0.5 \le T \le 8\ K$ considered, indicating occupation of the two lowest sublevels $n = 0,\ 1$. When T tends to zero, $\bar{\mu}$ approaches the Fermi levels $E_{1{\rm F}} = 4.98\ meV$ and $E_{2{\rm F}} = 2.28\ meV$, indicating that the electrons are highly degenerate.

In Fig. 1, we present the scaled resistances R/R_0 as a function of the temperature T in the range $4 \le T \le 8\ K$. Here, R_0 is the resistance R_1 due to surface roughness scattering at $T = 0.5\ K$. When only the roughness scattering is present, R_1 (dash-dot-dotted curve) increases with T due to gradual population ($\bar{\mu} \lesssim 2\hbar\Omega_0$) of the bottom of the sublevel $n = 2$, where the density-of-states (proportional to the inverse of the electron group velocity) is very large, yielding enhanced roughness scattering. When T is very high, R_1 becomes linear

in T. When phonon scattering is added, the total resistance R_2 (dashed curve) increases with T faster compared to R_1, causing an appreciable enhancement of the resistance at $T = 8\ K$. When electron-electron scattering is further included, R_3 (solid curve) displays a much stronger increase with T compared to R_2, showing a significant enhancement of the resistance at $T = 8\ K$. On the other hand, the differences among R_1, R_2, and R_3 become negligible at low temperatures $T \leq 1\ K$. The inset of the figure shows R_3/R_0 as a function of T in the whole range of T considered. The overall feature of R_3/R_0 reflects the T-dependence of R_1/R_0 since the system is dominated by roughness scattering.

Electron-electron scattering itself does not directly contribute to the resistance in the transport of electrons because it conserves the two-particle momentum through the scattering process. However, it contributes to the momentum dissipation indirectly by redistributing the electron energy. This point can be made clear by using Kohler's variational principle.[15,18] According to this theorem, the resistance is minimum and exact when the entropy production rate due to the external field is minimum. To make the argument simple, we suppose for a moment that the electron-electron interaction is infinitely large in comparison with other elastic and inelastic interactions. In this case, the exact resistivity is obtained when the transport relaxation time is independent of the energy in the effective-mass model. The exact resistivity is proportional to the entropy production rate under the DC field which vanishes for this solution.[18] What happens is that the electrons are swept through all possible accessible states rapidly by electron-electron scattering. As a result, the relaxation rate is averaged over these states and becomes independent of the energy. While this energy-independent relaxation rate minimizes the entropy production rate from electron-electron scattering and the resistance, this solution does not minimize the entropy production rate from other elastic and inelastic scattering mechanisms and raises the resistivity for these mechanisms beyond their original exact resistivity obtained in the absence of electron-electron scattering. In the presence of realistic (*i.e.,* finite) electron-electron scattering, there is a compromise between the electron-electron scattering and rest of the

scattering mechanisms in minimizing the entropy production rate, enhancing the net resistivity beyond the resistivity value without electron-electron scattering. Practically, the roughness scattering often dominates the phonon and electron-electron scattering at low temperatures, as seen in Fig. 1. However, we can theoretically highlight the importance of the buried electron-electron scattering either by deducting the contribution of roughness scattering or even by assuming the absence of roughness scattering in our system.

Figure 2 shows the effect of electron-electron scattering on the resistivity in the presence of strong roughness scattering in (a) and without roughness scattering in (b). Case (a) corresponds to the situation studied in Fig. 1 with the same definitions for R_1, R_2, R_3 but not for R_0. The contribution from the phonon or electron-electron scattering can be separated as clearly seen in (a) which presents the scaled resistance differences $\Delta R/R_0$ and in (b) which shows the scaled resistance R/R_0 as a function of the temperature. In (a), the contribution from phonon scattering is shown as $R_2 - R_1$ (dashed curve), while the contribution from electron-electron scattering is shown as $R_3 - R_2$ (solid curve). The phonon scattering part $R_2 - R_1$ displays a rapid rise above $T > T_0 = 2c_s\sqrt{2m^*(\bar{\mu} - \hbar\Omega_0)}/k_{\rm B} \sim 2.7$ K. The energy $k_{\rm B}T_0$ equals the energy of the phonon with wave number $q_y = 2k_{1\rm F}$ corresponding to the momentum transfer between the Fermi points in the sublevel $n = 1$. For $T \gg T_0$, $R_2 - R_1$ is found to exhibit a linear behavior in T/T_0. The electron-electron scattering contribution $R_3 - R_2$ vanishes at $T = 0$ K due to the restricted phase space available for scattering. However, $R_3 - R_2$ increases rapidly with T, roughly $\propto T^2$ below 2 K, a well-known behavior from the Umklapp scattering process.[18] In the high-temperature nondegenerate regime, we can show analytically that $(R_3 - R_2)/R_1$ approaches a constant $(4 - \pi)/\pi$ for the roughness-scattering dominated system in the presence of strong electron-electron scattering following the method given earlier by one of the authors.[15] In this high temperature regime, the increase of $R_3 - R_2$ slows down to a quasilinear dependence of R_1 as seen from (a). In contrast, we do not see the slow down in the increase of electron-electron scattering contribution with T at high temperatures in (b) in the absence of roughness

scattering. In this case, we can show analytically that the ratio of the upper solid curve and the lower dashed curve approaches a constant $4/\pi$ in the high-temperature nondegenerate regime for strong electron-electron interaction.[15] Interestingly, the numerical ratio of the resistance between the solid and dashed curves in (b) approaches roughly $4/\pi \simeq 1.3$ at high temperatures.

In the following we study the density dependence of the resistivity at $T = 4\ K$. The quantity $\bar{\mu}$ increases with n_{1D} from one range $0 < \bar{\mu} < \hbar\Omega_0$ to another range $\hbar\Omega_0 < \bar{\mu} < 2\hbar\Omega_0$, passing through the occupation of the bottom of sublevel $n = 1$ in the x direction at $n_{1D} = 0.5 \times 10^6\ cm^{-1}$. In Fig. 3, we show the calculated scaled resistances R/R_0 as functions of the density n_{1D} within a small range $0.8 \times 10^6 \leq n_{1D} \leq 1.0 \times 10^6\ cm^{-1}$. Here, R_0 is the resistance R_1 due to surface roughness scattering at $n_{1D} = 10^6\ cm^{-1}$. When only roughness scattering is present, the resistance R_1 (dash-dot-dotted curve) decreases with n_{1D} as $1/n_{1D}$. With phonon scattering added, we see very small changes in R_2 (dashed curve). When electron-electron scattering is further taken into account, we find relatively large changes in R_3 (solid curve) compared to that in R_2. In addition, the differences among R_1, R_2, and R_3 as functions of n_{1D} are smaller compared to those shown as functions of T in Fig. 1. The inset of the figure shows R_3/R_0 as a function of n_{1D} in the whole range of n_{1D} considered. The overall feature of R_3/R_0 in the inset is dominated by the roughness-scattering contribution R_1/R_0. The plateau-like feature in the range $0.4 \times 10^6 < n_{1D} < 0.6 \times 10^6\ cm^{-1}$ arises from the abrupt rise of R_1 near $n_{1D} = 0.5 \times 10^6\ cm^{-1}$, where $\bar{\mu}$ passes through the bottom of the $n = 1$ sublevel, where the scattering rate is very large due to the large density of states.

The dominance of roughness scattering in Fig. 3 overshadows the electron-electron scattering as a function of the electron density. Figure 4 highlights the effects of electron-electron and phonon scattering by (a) including and (b) removing the roughness scattering from our system. Case (a) corresponds to the situation studied in Fig. 3 with the same definitions for $R_1,\ R_2,\ R_3$ but not for R_0. The contribution from the phonon or electron-electron scattering can be separated as clearly seen in (a) which presents the scaled resistance differences

$\Delta R/R_0$ and in (b) which shows the scaled resistance R/R_0 as a function of the density. In (a), the contribution from phonon scattering is shown as $R_2 - R_1$ (dashed curve), while the contribution from electron-electron scattering is shown as $R_3 - R_2$ (solid curve). For phonon scattering in (a), $R_2 - R_1$ displays a broad peak around $n_{1D} = 0.5 \times 10^6\ cm^{-1}$ where the $n = 1$ sublevel starts to be populated. Just above the threshold density for the occupation of the $n = 1$ sublevel, the Fermi wave vector k_{1F} of this sublevel is small allowing efficient emission and absorption of small-momentum phonons. With further increasing of n_{1D}, k_{1F} becomes larger, leading to a suppression of phonon scattering or a decrease of $R_2 - R_1$ with n_{1D}. The electron-electron scattering contributions $R_3 - R_2$ vanishes in (a) at low density due to the complete cancellation of the intrasubband electron-electron scattering until the $n = 1$ sublevel is populated at $n_{1D} = 0.5 \times 10^6\ cm^{-1}$. When n_{1D} increases above this value, $R_3 - R_2$ increases dramatically with n_{1D} because more and more electrons are available for Coulomb scattering, in sharp contrast to the decrease of $R_2 - R_1$ with n_{1D}. As a result, $R_3 - R_2$ eventually dominates $R_2 - R_1$ above $n_{1D} > 0.8 \times 10^6\ cm^{-1}$. In the absence of roughness scattering, we find from (b) that the effect of electron-electron scattering (solid curve) is to enhance the phonon-scattering resistivity (dashed curve) above the threshold density at $n_{1D} = 0.5 \times 10^6\ cm^{-1}$. A completely different n_{1D} dependence of the resistance is seen in (b) for a roughness-free system in contrast with that in the inset of Fig. 3 for a roughness-dominated system.

V. CONCLUSIONS

In conclusion, we have investigated the effect of the electron-electron interaction on the resistance of diffusive electrons in a multi-sublevel single quantum wire as a function of the temperature and the density at low temperatures. The intrasubband electron-electron scattering is shown to have no effect. However, for systems with multi-sublevel occupation, electron-electron scattering is shown to enhance the resistance significantly. Also, this effect is relatively more important in high-density systems. We have demonstrated that this effect

can be studied with arbitrary accuracy using a formally exact solution of the Boltzmann transport equation in the presence of roughness and phonon scattering.

ACKNOWLEDGMENTS

Sandia is a multiprogram laboratory operated by Sandia Corporation, a Lockheed Martin Company, for the U.S. DOE under Contract No.DE-AC04-94AL85000.

REFERENCES

[1] J. Lee and H. N. Spector, J. Appl. Phys. **54**, 3921 (1983).

[2] G. Fishman, Phys. Rev. B **34**, 2394 (1986).

[3] H. Sasaki, T. Noda, K. Hirakawa, M. Tanaka, and T. Matsusue, Appl. Phys. Lett. **51**, 1934 (1987).

[4] S. Das Sarma and X. C. Xie, Phys. Rev. B **35**, 9875 (1987).

[5] K. F. Berggren, G. Roos, and H. van Houten, Phys. Rev. B **37**, 10118 (1988).

[6] H. Akira and T. Ando, Phys. Rev. B **43**, 11676 (1991).

[7] B. Tanatar and A. Gold, Phys. Rev. B **52**, 1996 (1995).

[8] S. K. Lyo and D. Huang, Phys. Rev. B **64**, 115320 (2001).

[9] T. Sugaya, J. P. Bird, M. Ogura, Y. Sugiyama, D. K. Ferry, and K. Y. Yang, Appl. Phys. Lett. **80**, 434 (2002).

[10] S. K. Lyo and D. H. Huang, Phys. Rev. B **66**, 155307 (2002).

[11] S. K. Lyo and D. H. Huang, Phys. Rev. B **68**, 115317 (2003).

[12] S. K. Lyo and D. H. Huang, J. Phys.: Condensed Matter **16**, 3379 (2004).

[13] R. W. Keyes, J. Phys. Chem. Solids **6**, 1 (1958), and references therein.

[14] J. Appel, Phys. Rev **122**, 1760 (1961).

[15] S. K. Lyo, Phys. Rev B **34**, 7129 (1986).

[16] D. H. Huang, P. M. Alsing, T. Apostolova, and D. A. Cardimona, Phys. Rev. B **71**, 195205 (2005).

[17] T. Holstein, Ann. Phys. (NY) **29**, 410 (1964).

[18] J. M. Ziman, *Electrons and Phonons*, (Oxford University Press, London, 1967), p. 277.

[19] S. K. Lyo, Phys. Rev. B **14**, 2335 (1976).

[20] D. H. Huang and S. X. Zhou, Phys. Rev. B **40**, 7750 (1989).

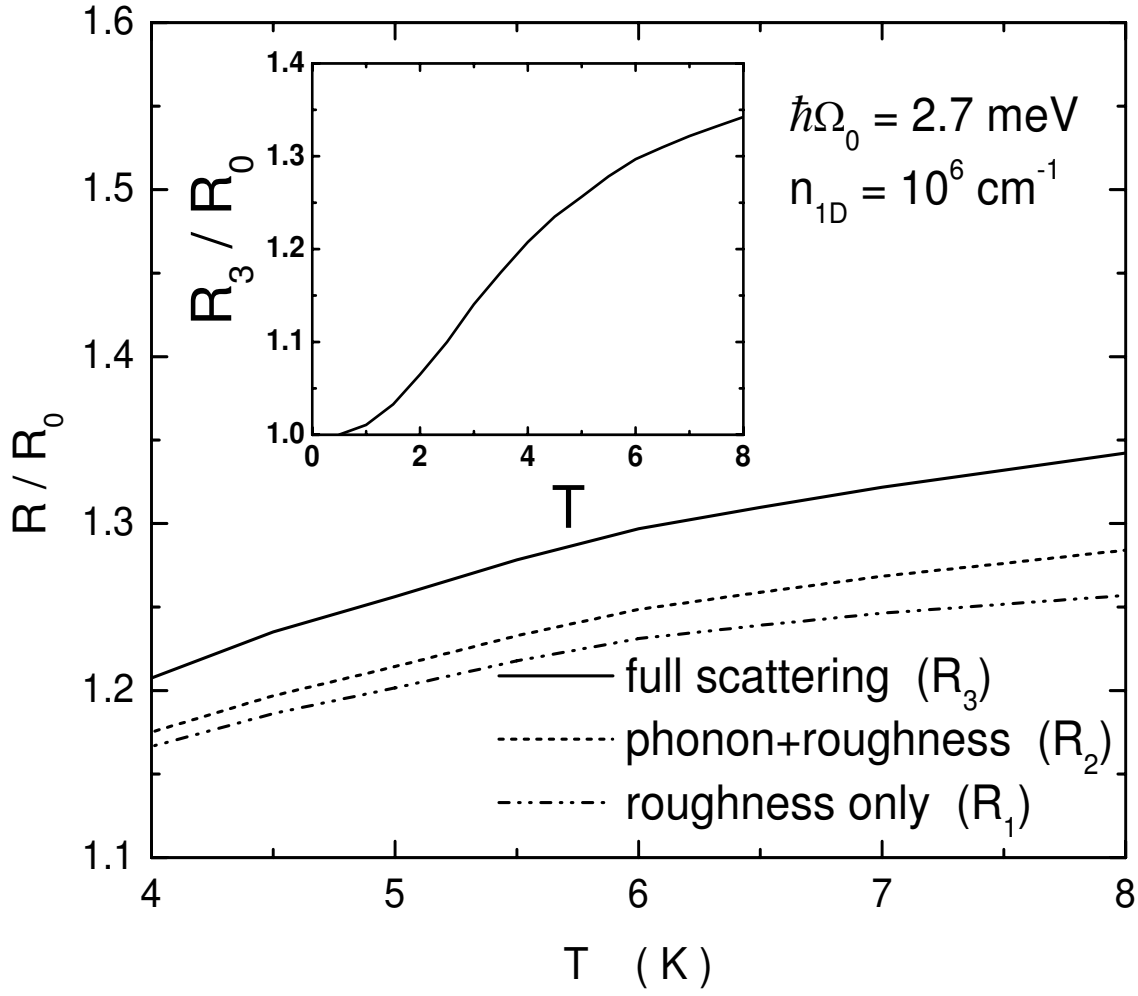

FIG. 1. Scaled resistances (R/R_0) as functions of the temperature T in the range $4 \leq T \leq 8\ K$. Here, $R_0 = 1.06\ (h/2e^2)$ is the resistance R_1 due to surface roughness scattering alone around $T = 0.5\ K$. Three different cases are compared to each other in the figure: (1) R_1 (dash-dot-dotted curve); (2) Roughness plus phonon scattering (R_2, dashed curve); (3) Roughness plus phonon plus electron-electron scattering (R_3, solid curve). The inset shows R_3/R_0 in the temperature range $0.5 \leq T \leq 8\ K$.

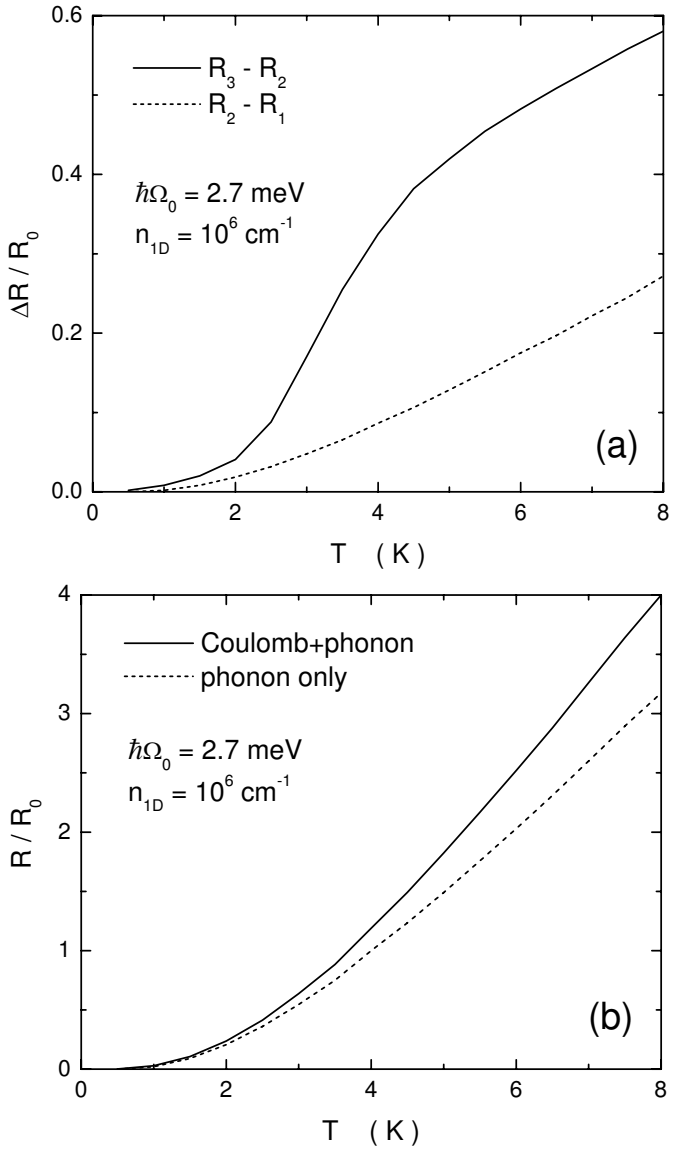

FIG. 2. Scaled resistance differences $\Delta R/R_0$ in (a) and the scaled resistance R/R_0 in (b) as functions of the temperature T. The roughness scattering is included in (a) but is excluded in (b). Case (a) corresponds to the situation studied in Fig. 1 with the same definitions for $R_1,\ R_2,\ R_3$ but not for R_0. Two different cases are compared to each other in (a) with $R_0 = 0.106\ (h/2e^2)$ and $L = 0.1\ \mu m$: (1) $R_2 - R_1$ (dashed curve, effect of phonon scattering); (2) $R_3 - R_2$ (solid curve, effect of electron-electron scattering). We have compared two results in (b) for phonon scattering only (dashed curve) and for combined electron-electron and phonon scattering (solid curve) with $R_0 = 0.678\ (h/2e^2)$ and $L = 100\ \mu m$.

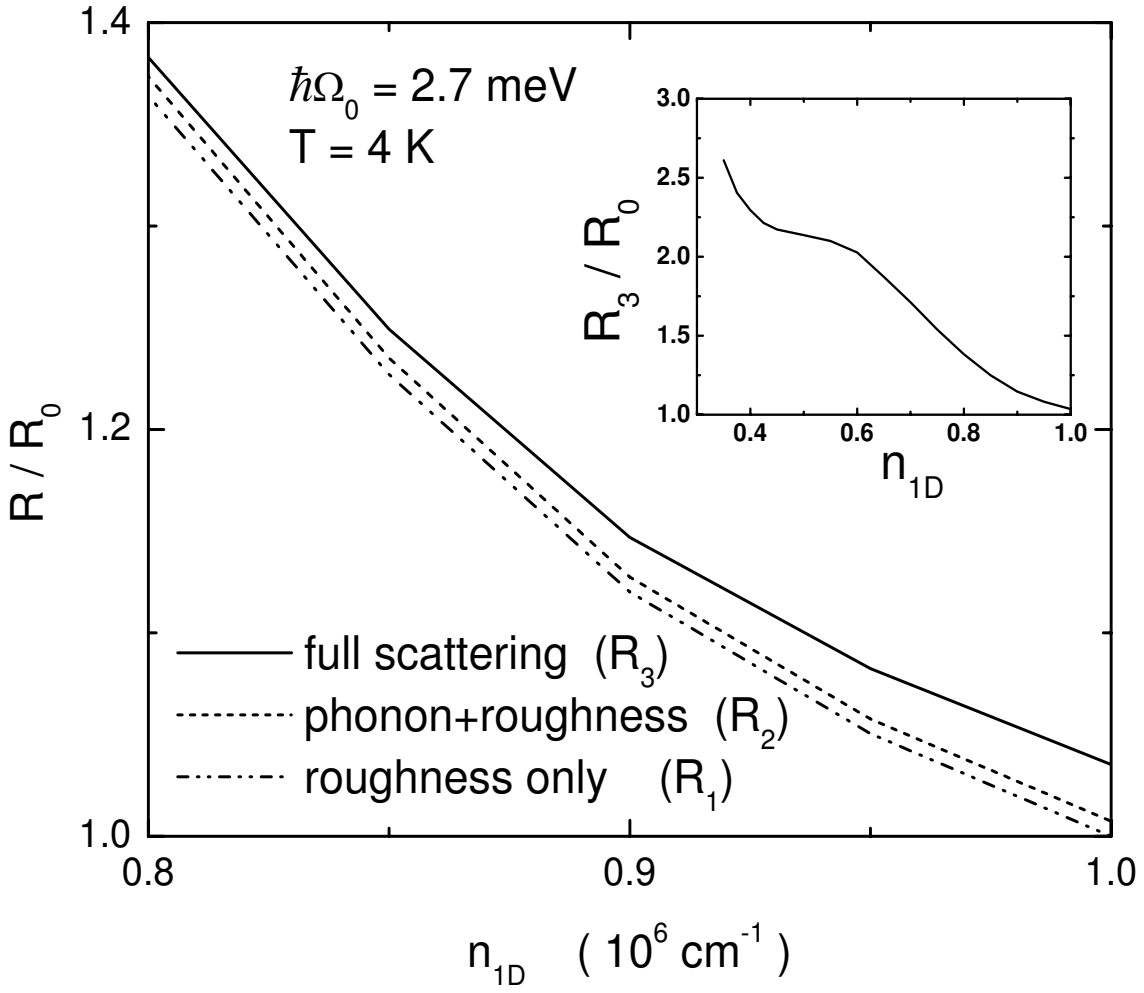

FIG. 3. Scaled resistances (R/R_0) as a function of the density $n_{1\mathrm{D}}$ in the range $0.8 \times 10^6 \leq n_{1\mathrm{D}} \leq 1.0 \times 10^6\ cm^{-1}$. Here, $R_0 = 1.236\ (h/2e^2)$ is the resistance R_1 due to surface roughness scattering alone at $n_{1\mathrm{D}} = 10^6\ cm^{-1}$. Three different cases are compared to each other in the figure: (1) R_1 (dash-dot-dotted curve); (2) Roughness plus phonon scattering (R_2, dashed curve); (3) Roughness plus phonon plus electron-electron scattering (R_3, solid curve). The inset shows R_3/R_0 in the range $0.35 \times 10^6 \leq n_{1\mathrm{D}} \leq 1.0 \times 10^6\ cm^{-1}$.

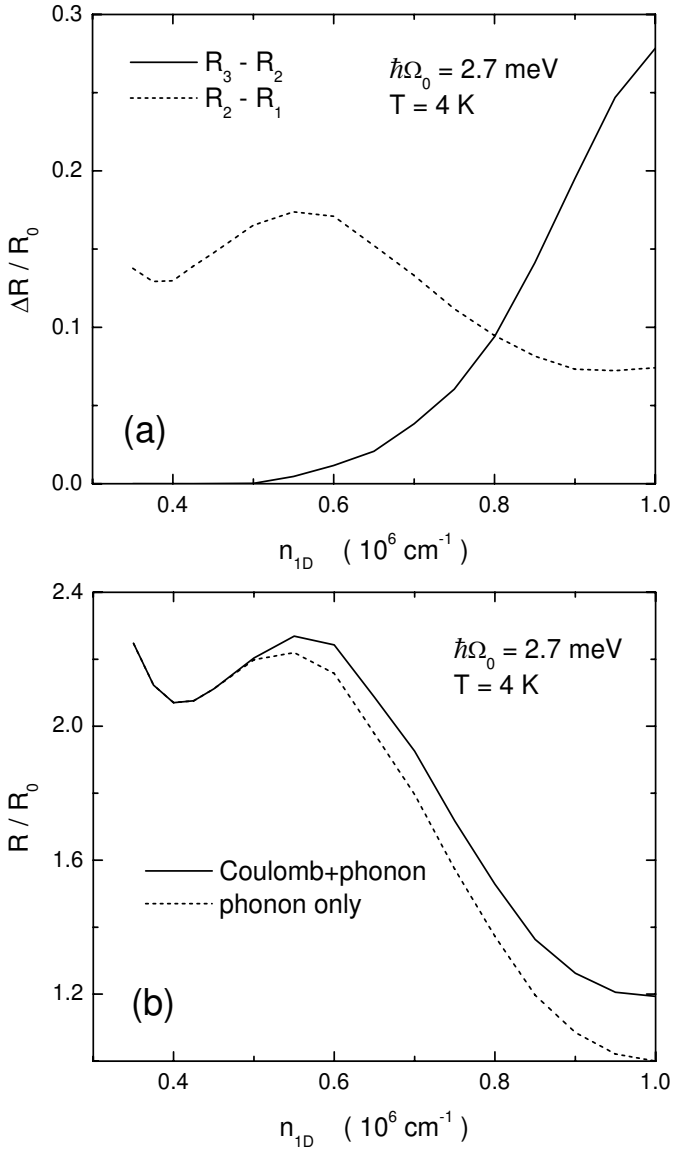

FIG. 4. Scaled resistance differences $\Delta R/R_0$ in (a) and the scaled resistance R/R_0 in (b) as a function of the density $n_{1\mathrm{D}}$. Roughness scattering is included in (a) but is excluded in (b). Case (a) corresponds to the situation studied in Fig. 3 with the same definitions for R_1, R_2, R_3 but not for R_0. Two different cases are compared to each other in (a) with $R_0 = 0.124$ $(h/2e^2)$ and $L = 0.1$ μm: (1) $R_2 - R_1$ (dashed curve, effect of phonon scattering); (2) $R_3 - R_2$ (solid curve, effect of electron-electron scattering). We have compared two results in (b) for phonon scattering only (dashed curve) and for combined electron-electron and phonon scattering (solid curve) with $R_0 = 0.667$ $(h/2e^2)$ and $L = 100$ μm.